ACS OMEGA

http://pubs.acs.org/journal/acsodf

Article

Oxy-Combustion of Solid Recovered Fuel in a Semi-Industrial CFB Reactor: On the Implications of Gas Atmosphere and Combustion Temperature

Joseba Moreno,* Max Schmid, Steven Scharr, and Günter Scheffknecht

Cite This: *ACS Omega* 2022, 7, 8950−8959

Read Online

ACCESS | Metrics & More | Article Recommendations

ABSTRACT: Oxy-fuel combustion of refuse waste is gaining considerable attention as a viable CO_2 negative technology that can enable the continued use of stationary combustion plants during the transition to renewable energy sources. Compared to fossil fuels, waste-derived fuels tend to be highly heterogeneous and to contain a greater amount of alkaline metals and chlorine. Therefore, experimental studies are mandatory to thoroughly elucidate refuse materials' combustion and pollutant formation behavior. This paper presents an experimental investigation on the air and oxy-fuel combustion of solid recovered fuel at a 200 kW_{th} circulating fluidized bed facility. In the course of two experimental campaigns, the effects of combustion atmosphere and temperature on pollutant formation (i.e., NO_x, SO_2, and HCl) and reactor hydrodynamics were systematically studied. In contrast to air-firing conditions, the experimental results showed that oxy-fuel combustion enhanced the volume concentration of NO_x by about 50% while simultaneously decreasing the fuel-specific NO_x emissions (by about 33%). The volume concentrations of SO_2 and HCl were significantly influenced by the absorption capacity of calcium-containing ash particles, yielding corresponding values close to 10 and 200 ppmv at 871−880 °C under oxy-fuel combustion conditions. In addition, the analysis of hydrodynamic data revealed that smooth temperature profiles are indispensable to mitigate bed sintering and agglomeration risks during oxy-fuel operation. The results included in this study provide a valuable contribution to the database of experimental information on the oxy-fuel combustion of alternative fuels, which can be applied in future process model validations and scale-up studies.

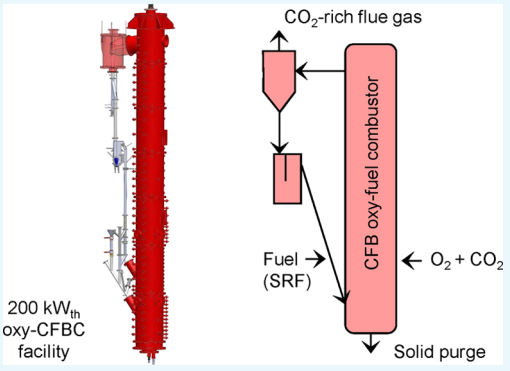

1. INTRODUCTION

Climate change mitigation and sustainable waste management are among the most important societal challenges recognized by the 2015 Paris Climate Agreement[1] and the European Union Action Plan for a Circular Economy Package.[2] The thermal valorization of refuse waste (e.g., incineration and co-combustion) has gained increasing popularity in recent years as a solution for decreasing the volume of solids disposed of in landfills, and thereby the associated greenhouse gas emissions. Still, the intrinsic fuel characteristics (e.g., form and particle size and ash and moisture content) must be carefully evaluated during the process design step to ensure reliable plant operation and effective emissions control.

Due to their high fuel adaptability, increased solid residence time, and low pollutant emission, circulating fluidized bed (CFB) systems are particularly well suited for the combustion of low-grade fuels. Moreover, CFB systems can be applied within the framework of carbon capture and storage (CCS) technologies to capture CO_2 from power and industrial sources. In parallel, the combination of CCS with non-conventional fuels enables the achievement of net negative emissions by sequestration of biogenic CO_2. The latter approach is often referred to as bioenergy with carbon capture and storage (BECCS) and is expected to play a major role in meeting the 2050 zero-carbon emissions target.[1,3−6]

In the last few decades, oxy-fuel combustion has evolved into one of the leading technologies considered for capturing CO_2 from power plants with CCS. The process consists of burning fuel with nearly pure oxygen instead of air (see Figure 1).

The justification for using oxy-fuel is to generate a flue gas with a high concentration of CO_2 and water vapor and then separate the CO_2 from the flue gas by dehydration and low-temperature purification processes. Consequently, the oxy-fuel combustion for power generation typically consists of the following major units: (i) an air separation unit (ASU) for

Received: December 28, 2021
Accepted: February 10, 2022
Published: March 2, 2022

https://doi.org/10.1021/acsomega.1c07334
ACS Omega 2022, 7, 8950−8959

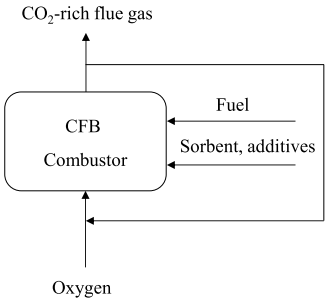

Figure 1. Simplified scheme of the oxy-fuel combustion process.

oxygen production; (ii) a boiler or gas turbine for combustion of fuel and generation of heat; and (iii) a CO_2 processing unit (CPU) for final purification of the CO_2 prior to utilization or storage. With the purpose of controlling the flame temperature, part of the flue gas is recycled back into the boiler. In addition, the process offers the possibility to comprehensively reduce the amount of SO_x in the flue gas and mitigate adverse effects such as slagging and fouling in heat exchanger surfaces. The latter is achieved by continuous addition of sorbents (e.g., limestone) and additives (e.g., aluminosilicates), respectively. To date, the oxy-CFB process has been widely studied in bench-scale and pilot-scale facilities. The tested fuels have usually been fossil fuels,[7−9] although biomass and sewage sludge have also been applied in some units.[10−12] Recently, waste-derived fuels [e.g., solid recovered fuels (SRF)] have started to play a key role in the energy sector due to the excessive depletion of non-renewable sources. At the time of writing, several studies have been reported on the oxy-fuel CFB co-firing characteristics of biomass waste fuels with coal.[13,14] Moreover, a recent work by Haaf et al. has demonstrated the feasibility of standalone SRF oxy-fuel combustion at a semi-industrial CFB facility.[15]

Besides, oxy-fuel combustion may affect the emissions of particular gas pollutants. As compared with air-firing, oxy-fuel tends to increase the volume concentration of NO_x in the flue gas while simultaneously reducing the mass of NO_x released per energy generated.[7,16] The increased NO_x concentrations during oxy-fuel operation are usually ascribed to a significant reduction in the combustion flue gas volume flow, caused by the absence or airborne nitrogen.[17,18] Concurrently, (thermal) NO_x formation is greatly inhibited in oxy-CFB boilers due to the moderate combustion temperature and the staged oxidant addition.[19,20] However, elevated oxy-fuel levels might promote thermal NO_x formation due to the presence of localized hot spots resulting from the more intense combustion conditions.[21] Consequently, the design of an efficient oxy-fuel CFB furnace deserves considerable attention because it needs to be balanced by the criteria of operational conditions (i.e., sufficient gas flow rates) and process economics (i.e., CAPEX and OPEX savings).

HCl is another critical component in utility boilers using alternative fuels, as elevated emissions of HCl are well known to cause major operational issues such as slagging, fouling, and corrosion.[22] At high temperatures, alkali metals (M) and chlorine (Cl) are released from the fuel into the flue gas as vaporized alkali metal chlorides (MCl). In the following, the sulfation process transforms alkali chlorides into alkali sulfates (M_2SO_4) under the effect of humid sulfur species, releasing chlorine as HCl (please refer to ref 23 for more details)

$$2MCl + SO_2 + H_2O + 1/2O_2 \rightarrow M_2SO_4 + 2\,HCl \quad (1)$$

$$2MCl + SO_3 + H_2O \rightarrow M_2SO_4 + 2\,HCl \quad (2)$$

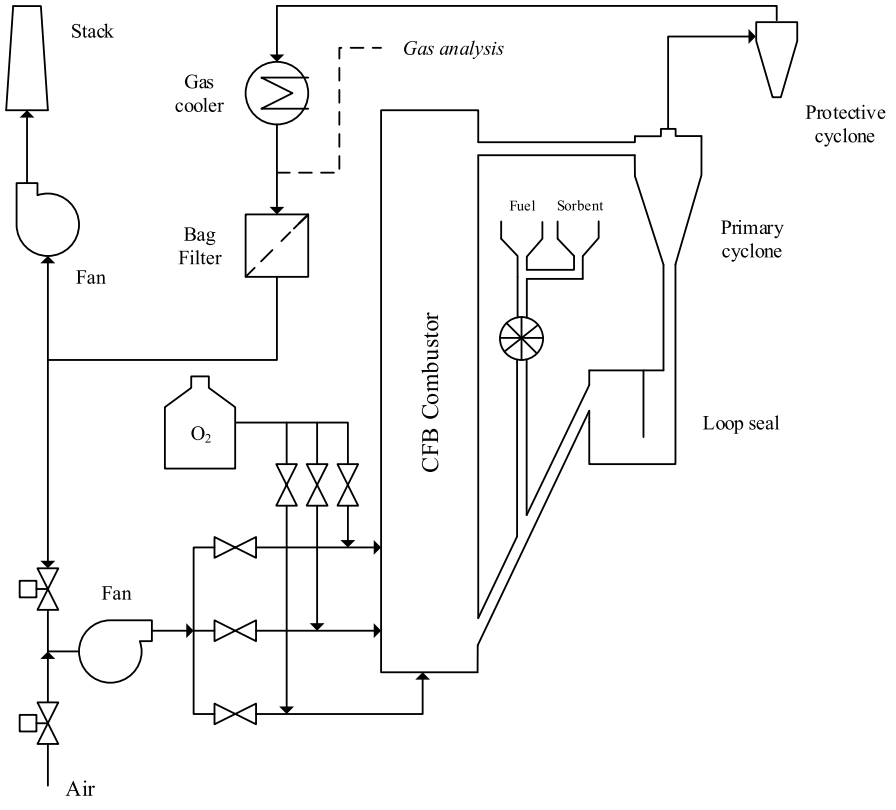

Figure 2. Schematic of the University of Stuttgart's 200 kW_{th} oxy-fuel CFB combustion facility.

https://doi.org/10.1021/acsomega.1c07334
ACS Omega 2022, 7, 8950−8959

Table 1. Chemical Composition of the Utilized Fuel

	γ_C	γ_H	γ_O	γ_N	γ_S	γ_{Cl}	γ_{ash}	γ_{H_2O}
	kg/kg, waf						kg/kg, wf	kg/kg, ad
Remondis SBS1	0.547	0.074	0.345	0.027	0.002	0.005	0.094	0.114

At the time of writing, only a few studies have been reported on evaluating the HCl emission characteristics during the combustion of non-conventional fuels. Xie and Ma evaluated the HCl emission behavior when firing eucalyptus bark at various temperatures.[24] In contrast, Hou et al. explored the HCl emissions arising from sewage sludge combustion in a CFB unit.[25] More recently, the fate of chlorine during oxy-CFB combustion of SRF has been addressed at the pilot scale.[15]

This work examines the combustion behavior of SRF under conditions prevailing in modern waste CFB incinerators. In this study, we evaluate the impact of combustion atmosphere (i.e., air and oxy-fuel) and temperature (i.e., 840−924 °C) on gaseous emissions (i.e., NO_x, SO_2, and HCl) and reactor hydrodynamics. The experiments were carried out at the University of Stuttgart's 200 kW_{th} CFB pilot plant, under conditions typical of industrial operation (i.e., recirculated flue gas and technically pure oxygen). The evaluation of ash formation and deposition behavior is beyond the scope of this work.

2. METHODOLOGY AND VALIDATION

2.1. Experimental Section. The University of Stuttgart's 200 kW_{th} pilot facility consists of three refractory-lined fluidized bed reactors connected by a solid flow transport system.[26,27] For the experimental investigations included in this study, the CFB combustion facility was employed. Figure 2 gives a schematic representation of such installation.

The fully refractory-lined CFB riser is 10 m high and has an average inner diameter of 200 mm. The reactor is connected to a high-efficiency primary cyclone, which separates the flue gas and the solids entrained from the system in a preliminary step. The exhaust gas is then passed through a protective (i.e., secondary) cyclone for fly ash and dust removal. After subsequent cooling, the off-gas undergoes particle clean-up in a baghouse filter before being partly recirculated to the riser inlet or vented to the environment by means of an induced draft fan. The CFB boiler is capable of operating in air-blown, oxygen-enriched, or oxy-combustion mode. The oxidant can be fed in three stages for smooth control of boiler temperature and pollutant formation. In addition, the chamber temperature might be balanced by means of a top heat exchanger. The feeding of solids (i.e., fuel and sorbent) is achieved by gravimetrically controlled screw feeders. Concurrently, bottom ash can be discharged by means of a bottom drain valve. Solid samples can be collected from the loop seal (i.e., circulating fraction) and from fly ash and bottom ash discharge points, respectively. The off-gas composition is continuously monitored using diverse methods such as non-dispersive infrared spectroscopy (CO, CO_2, SO_2, and NO_x), paramagnetism (O_2), and impact jet psychrometry (H_2O). In addition, a Fourier-transform infrared spectrometer can be employed to measure other gas species of interest (e.g., HCl).

The chemical composition of the fuel utilized in this work is given in Table 1. The latter consists of high calorific fractions separated from bulky and household waste (SBS1, REMONDIS GmbH & Co. KG, Region Rheinland, Germany) intentionally prepared to meet quality requirements such as a calorific value and mercury or chlorine content.[28] To guarantee adequate SRF dosing in the pilot facility, a procedure for conditioning the SBS1 was developed. The process consisted of mechanical steps such as shredding, briquetting, and subsequent shredding. Besides, Table 2 shows the chemical composition of the sorbent used in the pilot experiments. The silica sand DORSILIT 9 was delivered from Gebrüder Dorfner GmbH & Co. Kaolin-und Kristallquarzsand-Werke KG in the size range of 100−400 μm.

Table 2. Chemical Composition of the Utilized Bed Material

	x_{SiO_2}	$x_{Al_2O_3}$	$x_{Fe_2O_3}$	x_{H_2O}	x_{others}
	kg/kg, wf				
DORSILIT 9	0.95	0.025	0.0004	0.023	0.0016

2.2. Evaluation Methodology. There are multiple ways to express the concentration of a pollutant in the flue gas. In the following, the different approaches considered throughout this publication are briefly explained:

- y_i (ppmv): the volume concentration of a trace component "i" in the off-gas is expressed in parts-per-million. y_{NO_x} and y_{SO_2} are introduced in dry conditions, while y_{HCl} is given on a wet basis.
- e_i (mg/MJ_{th}): the emission factor of a trace component "i" is defined as the mass of pollutant released per energy generated

$$e_i = \frac{\dot{M}_i}{\dot{Q}_{th,H_u}} = \frac{\dot{V}_{FG,STP} \cdot y_i \cdot \rho_{n,i}}{H_u \cdot \dot{M}_B} \quad (3)$$

where the mass flow ($\dot{M}_i$) is the product between the flue gas volume flow at standard temperature and pressure conditions ($\dot{V}_{FG,STP}$), and the volume fraction (y_i) and standard density ($\rho_{n,i}$) of the gas pollutant "i". In parallel, $\dot{Q}_{th,H_u}$ refers to the CFB combustor's thermal duty based on the fuel's mass flow rate ($\dot{M}_B$) and net calorific value (H_u).

- c_i (mg/m^3): the mass concentration of a trace component "i" in the flue gas can also be expressed in metric units according to the following equation

$$c_i = \frac{\dot{M}_i}{\dot{V}_{FG}} = \frac{\dot{V}_{FG,STP} \cdot y_i \cdot \rho_{n,i}}{\dot{V}_{FG,STP}} \quad (4)$$

In addition, it might be of particular interest to calculate the conversion rate (η_i) of certain fuel elements during the combustion process according to the measured concentration as follows

$$\eta_i = \frac{\dot{M}_i}{\dot{M}_B \cdot \gamma_i} = \frac{\dot{V}_{FG,STP} \cdot y_i \cdot \rho_{n,i}}{\dot{M}_B \cdot \gamma_i} \quad (5)$$

https://doi.org/10.1021/acsomega.1c07334
ACS Omega 2022, 7, 8950−8959

where γ_i indicates the mass fraction of component "i" in the fuel.

3. RESULTS AND DISCUSSION

The overall goal of this study was to explore the CFB combustion characteristics of SRF under process conditions similar to those envisaged in modern waste incinerators. The results presented in this work are related to the CFB combustor's performance under different oxidizing gas atmospheres and process temperatures, so as to derive implications on pollutant formation and hydrodynamic stability.

Each experiment was operated for at least 1 h (although in general 2 h) after steady-state conditions were reached. In addition, selected tests were conducted for longer operational times to assess the process performance on a longer-term basis. In the course of the presented experiments, the pilot facility was operated over a wide operating range (see Table 3). While the reactor inventory was maintained roughly constant (i.e., 1005−1238 kg/m^2 or 32−39 kg), the process temperature was varied between 840 and 924 °C to derive implications on the overall process performance. During oxy-fuel combustion, two different inlet oxygen concentrations were investigated, namely, 28 vol % (OXY28) and 35 vol % (OXY35). Both oxy-fuel cases were established by adjusting the amount of recirculated flue gas, which averaged 87 and 74%, respectively. An even higher oxy-fuel level (i.e., OXY45) has been recently demonstrated at the 200 kW$_{th}$ oxy-CFB combustion facility and will be discussed in a separate work. Air-firing experiments yielded considerably higher gas superficial velocities (up to 6.5 m/s) due to the increased gas flow throughput. Nevertheless, the observed differences in u_0 posed a minor effect on the system's hydrodynamics as stable and sufficient internal solid circulation could be attained in both operation modes. Besides, the oxidant staging level was kept constant in the course of the experimental investigations.

Table 3. Experimental Range of Operating Conditions

parameter	symbol	value/range	unit
heat duty	$\dot{Q}_{th}$	106−154	kW
temperature	T	840−924	°C
stoichiometric oxygen-to-fuel ratio	ξ	1.0−2.0	kg/kg
inlet oxygen concentration	$y_{O_2,in}$	21−35	vol %
oxidant staging (prim./sec./tert.)		40/30/30	%
gas superficial velocity	u_0	3.9−6.5	m/s
flue gas recirculation rate	ν	48−58	%
solid inventory	W_s	1005−1238	kg/m^2

3.1. Material Balance Closure. The reactor material balance was assessed within the first phase of the experimental evaluation using measured plant data such as gas concentrations, volume flows, and solid flows. Elementary combustion equations were employed to assess the experimental results' quality by estimating the flue gas composition and off-gas volume flow. The latter calculations were performed using stoichiometric relations and assuming complete fuel combustion. Figure 3 displays the comparison between the calculated and measured plant data. The depicted circles correspond to oxy-fuel combustion conditions, while the triangles indicate values obtained during air-firing. The calculated CO_2 and O_2 concentrations correlate well with the measured values, indicating a satisfactory closure of the combustor material balance. Deviation of the measured and calculated values for such gas components averaged 0.9 and 6%, respectively. Besides, the calculated and measured steam volume fractions introduce a higher dispersion (up to 18%), which can be associated with model simplifications and assumptions (e.g., constant moisture content of the fuel) in combination with instrument errors. The measured and calculated off-gas volume flows yielded a maximum deviation of 6.3%. The latter disparity can be regarded as marginal, considering the modest flue gas duct's cross section and the impeller anemometer's accuracy within the measured volume flow range.

3.2. Gaseous Emissions. The combustion conditions defined in a boiler have a crucial influence on the emissions of the diverse gas species. Low combustion efficiencies resulting in high energy wastage and increased pollutant emissions are mainly ascribed to an insufficient oxygen amount in the oxidant supply (i.e., inadequate oxygen ratio, ξ) and poor mixing between air and fuel.[29,30] Generally, efficient oxy-combustion of coal is achieved with stoichiometric relations

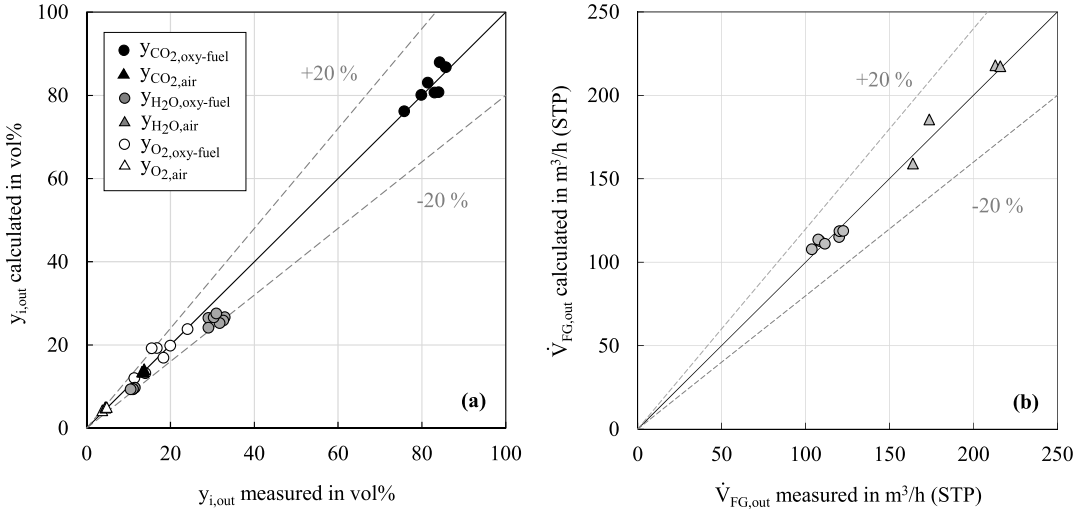

Figure 3. Comparison of the combustor material balance for calculated and measured flue gas concentrations (y_i) (a) and flue gas volume flow ($\dot{V}_{FG}$) (b).

https://doi.org/10.1021/acsomega.1c07334
ACS Omega 2022, 7, 8950−8959

ranging between 1.05 and 1.15.[31,32] Nonetheless, complete combustion of biomass and waste-derived fuels (e.g., SRF) requires increased stoichiometric oxygen-to-fuel ratios to compensate for the relatively high volatile fraction and the large inhomogeneity of biogenic fuels.[33,34] The results, presented in Figure 4, corroborate the last assertion. At the

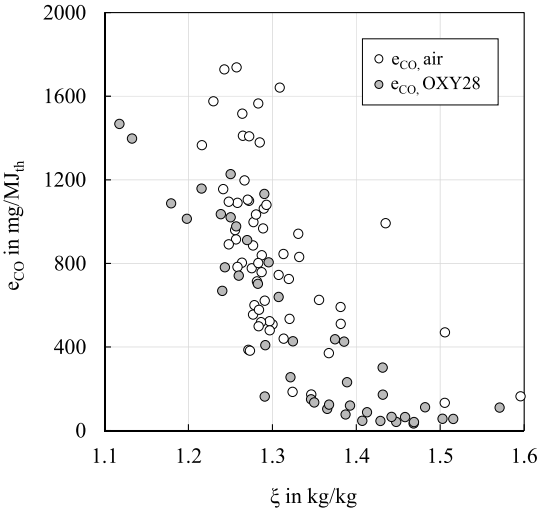

Figure 4. CO emission factor (e_{CO}) *vs* stoichiometric oxygen-to-fuel ratio (ξ) during air-firing and oxy-fuel combustion conditions.

200 kW_{th} CFB combustion facility SBS1 was combusted over a wide range of stoichiometric oxygen-to-fuel ratios both during air and oxy-fuel firing conditions. The results indicate that a minimum stoichiometric-to-fuel ratio of 1.4 is required in both cases to drive CO emissions below a mark of 100 mg/MJ_{th}, which corresponds roughly to an emission limit of 250 mg/m^3 imposed on non-woody biofuel German combustion plants with a total capacity up to 100 MW.[35] The latter finding is also in line with the observations made by Haaf et al. in a recent study, where ξ values between 1.3 and 1.6 were proposed to ensure adequate burnout of SRF in an oxy-fuel CFB combustion unit.[36]

3.2.1. NO_x. Nitrogen oxides (NO_x) represent a potential corrosion risk in the processing of CO_2 from oxy-fuel combustion processes due to the formation of nitric acid.[37] Figure 5 introduces the fuel-specific NO_x emission factor (a) and the NO_x volume concentration (b) against the stoichiometric oxygen-to-fuel ratio, both during air and oxy-fuel firing conditions.

The NO_x concentration during oxy-fuel combustion tends to be higher than during air firing conditions due to (i) gas pollutants enrichment through flue gas recirculation and (ii) the increased amount of oxygen in the oxidizer. At the same time, fuel-specific NO_x emissions are generally lower in the oxy-fuel case mainly because of (i) the low nitrogen environment in combination with (ii) the reduction in the total flue gas flow. The findings of this study support both assertions. Figure 5a indicates that the mass of NO_x released per energy generated during oxy-fuel was up to 33% lower than during the air-combustion case. Concurrently, the NO_x volume fraction measured during oxy-fuel was about 50% higher than the NO_x concentration measured during air combustion conditions. The attained NO_x emissions during oxy-fuel SRF combustion are similar to the values reported by Haaf et al., 2020 in a recent study.[15] Furthermore, the decrease in NO_x emissions observed during oxy-fuel experiments is comparable to the reduction extent reported in other oxy-combustion studies (i.e., 20−70%).[38,39] The linearity of NO_x formation with excess oxygen has already been postulated in previous works.[19,20] The latter behavior can be attributed to a decreased reducing zone in the combustor, which results in the reduction of NO_x to N_2.[40] In addition, Figure 5 facilitates the reading of the fuel-N conversion ratio (a) and the mass concentration of NO_x (b) in both combustion experiments. In agreement with the observations made by other authors, air combustion leads to a higher nitrogen conversion than oxy-fuel combustion.[41,42] Under adequate fuel burnout conditions (i.e., $\xi \approx 1.4$), fuel-nitrogen to NO_x ratios between 6 and 7.1% were calculated, while air-firing experiments yielded values between 8 and 8.7%.

The combustion temperature is another major variable that influences the fuel's conversion degree and thus, the combustion flue gas composition. Figure 6 introduces the concentration of NO_x for all conducted experiments against the reactor temperature. Please note that due to the very similar excess oxygen levels measured in the flue gas a correction to a reference O_2 value is not required in this work. Compared to air-firing, the graph indicates that NO_x levels are

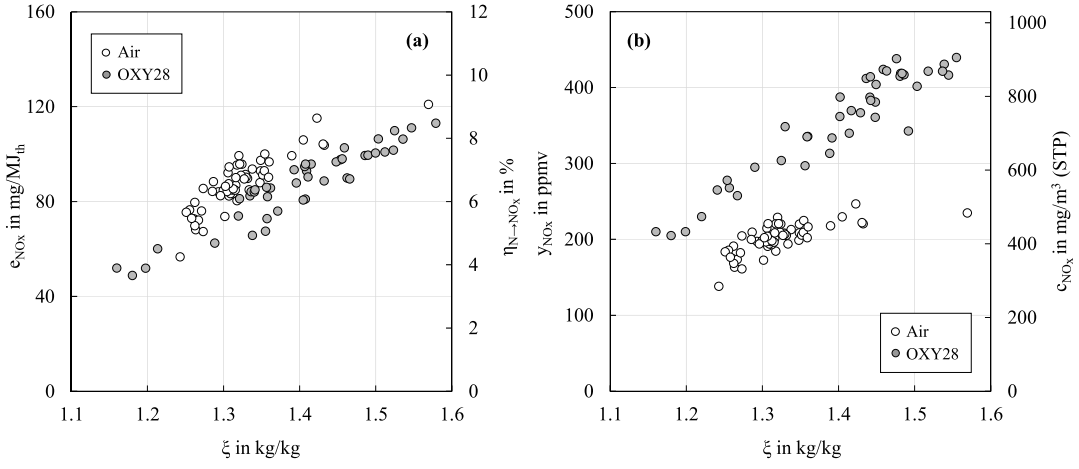

Figure 5. (a) NO_x emission factor (e_{NO_x}) and fuel-N to NO_x conversion ratio ($\eta_{N\rightarrow NO_x}$) *vs* stoichiometric oxygen-to-fuel ratio (ξ). (b) NO_x concentration (y_{NO_x}, c_{NO_x}) *vs* stoichiometric oxygen-to-fuel ratio (ξ).

https://doi.org/10.1021/acsomega.1c07334
ACS Omega 2022, 7, 8950−8959

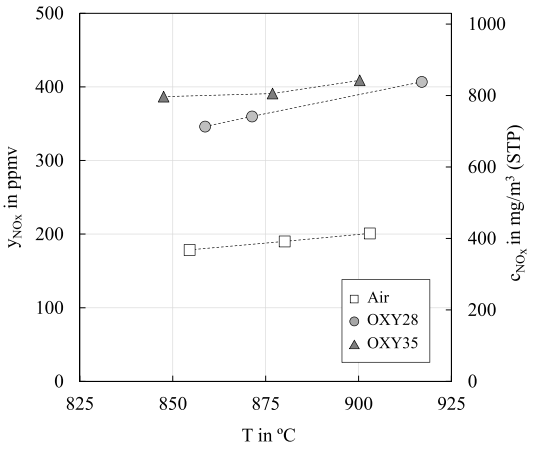

Figure 6. NO_x concentration (y_{NO_x}, c_{NO_x}) *vs* reactor temperature (T) for all the investigated air and oxy-fuel combustion experiments.

substantially promoted during oxy-fuel combustion. With a target boiler temperature of 860 °C, 179 ppmv were measured during air-firing conditions. Concurrently, 346 ppmv were yielded at an inlet oxygen concentration of 28 vol % and a similar temperature. Within the same combustion setting, the reactor temperature showed a marginal influence on y_{NO_x}, indicating a slightly increasing tendency in all the investigated cases.[9] The latter finding correlates well with the observations made by Hofbauer, who postulated that NO_x levels are not necessarily promoted at higher process temperatures as long as a uniform temperature profile over the furnace is attained.[7] In any case, the results presented in this section show that, depending on the required CO_2 specifications, an oxy-fuel CFB combustor utilizing SRFs of similar quality will most probably require a NO_x removal step before the CO_2 processing unit. Nitrogen oxides, on the other hand, can be easily removed through CPU compression.[37] The conversion of NO_x to NO_2 is favored at increased pressures. Concurrently, NO_2 has high solubility, allowing it to form nitric acid by dissolving NO_2 in water, following compression at around 30 bar in an absorption column.

3.2.2. Acidic Gases (i.e., SO_2 and HCl). Generally, biomass and fuels with increased biogenic share (e.g., SRF) are characterized by a lower sulfur content than most coals, reducing fuel-related SO_2 emissions responsible for acidification.[13,43] However, the sulfur amount in the fuel can play an essential role in sulfating alkali chlorides, which are known for enhancing deposit formation and accelerating superheater corrosion. The influence of combustion atmosphere (a) and process temperature (b) on the evolution of SO_2 and HCl concentrations is introduced in Figures 7 and 8, respectively. Figure 7a indicates that SO_2 emissions tend to decrease with increasing ξ (i.e., fuel-rich region) and might be attributed to alkali species in ash that favor sulfur retention.[44] Furthermore, the trend of SO_2 introduced in Figure 7a aligns well with the observations made by Hu et al., who reported a decrease in SO_2 emissions with equivalence ratios higher than 1.2, both during air and oxy-fuel combustion conditions.[45] Figure 7b presents the dependency of SO_2 volume concentration from the process temperature. According to the illustration, there is a temperature range in which SO_2 is remarkably suppressed. As indicated by Spörl et al., the latter behavior can be explained by the presence of calcium-containing species in the fuel ash, which can bind SO_2 according to different routes.[46] Moreover, the proposed temperature range in this study (i.e., 871−880 °C) correlates well with the observations made by Díez et al., who reported maximum SO_2 retention values when operating in a temperature window between 880 and 890 °C.[47]

Compared to air-firing conditions, HCl emissions are particularly promoted during oxy-fuel combustion due to enhanced metal vaporization and chlorination achieved by flue gas recirculation.[48] The results depicted in Figure 8a corroborate the latter assertion. The specific HCl emissions at oxy-fuel conditions were over three times higher than those measured during the air-firing experiment. Also, Allgurén and Andersson reported a comparable trend in a recent study.[49] The authors also attributed the effect to flue gas recirculation, indicating a higher concentration of sulfuric species during oxy-fuel than in the air-firing case. Besides, the results depicted in Figure 8a indicate that excess oxygen (i.e., stoichiometric ratio) does not pose a substantial effect on HCl. As HCl is not an oxidation product, any minor variations in e_{HCl} can be explained by little differences in the fuel mass flow rate. Furthermore, HCl can react with O_2 at high oxy-fuel levels, generating chlorine and water vapor via the exothermic Deacon reaction.[50] Nonetheless, in the current investigation,

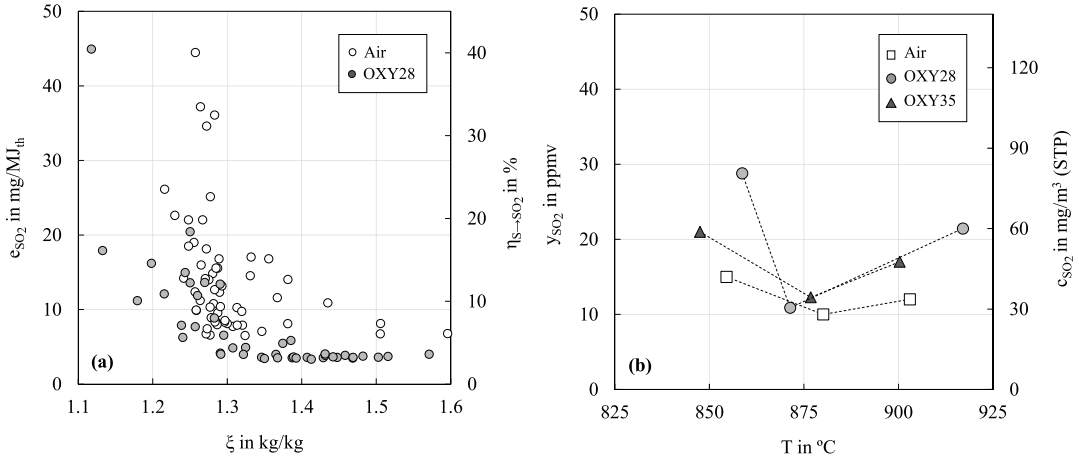

Figure 7. (a) SO_2 emission factor (e_{SO_2}) and fuel-S to SO_2 ratio ($\eta_{S\rightarrow SO_2}$) *vs* stoichiometric oxygen-to-fuel ratio (ξ). (b) SO_2 concentration (y_{SO_2}, c_{SO_2}) *versus* reactor temperature (T).

https://doi.org/10.1021/acsomega.1c07334
ACS Omega 2022, 7, 8950−8959

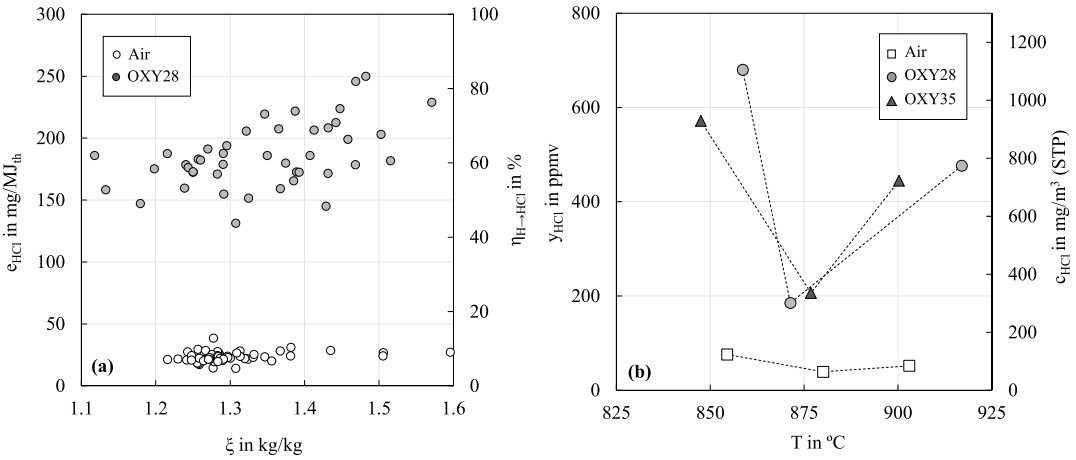

Figure 8. (a) HCl emission factor (e_{HCl}) and fuel-H to HCl ratio ($\eta_{H\rightarrow HCl}$) *vs* stoichiometric oxygen-to-fuel ratio (ξ). (b) HCl concentration (y_{HCl}, c_{HCl}) *vs* reactor temperature (T).

the latter reaction was assumed to play a minor role, considering the comparably high boiler temperatures that will cause the equilibrium to shift toward the reactants, lowering the conversion of HCl to Cl_2. The influence of temperature on HCl is presented in Figure 8b. According to Hou et al., an elevated HCl concentration with temperature might be expected as a result of the increased gas partial pressure of metal chlorides.[25] The temperature limits depicted in Figure 8b support partly the latter observation. However, there is a sharp decrease in y_{HCl} in the range between 871 and 880 °C that can be attributed to a decreased availability of SO_2 to form HCl according to eq 2 in combination with the ability of CaO to absorb HCl under conditions typical for fluidized bed combustors.[50] In any case, it becomes evident that the HCl emissions yielded during SRF CFB combustion will require subsequent treatment to comply with the emission limit set by the Industrial Emissions Directive (i.e., 2−8 mg/m^3).[51] Among the different methods included in the best available techniques (BATs), dry sorbent injection (DSI) is particularly well suited due to its simplicity, exceptionally high removal efficiency, and low environmental impact. Nonetheless, the potential of DSI for the fluidized bed application has not been fully assessed. Therefore, further research is still required to validate the latter observation.

3.2.3. Hydrodynamic Behavior. Figure 9a introduces the temperature and pressure profiles of the 200 kW$_{th}$ oxy-fuel reactor during the conducted air-firing and oxy-fuel tests at a reference temperature of 880 °C. The riser height refers to the wind box nozzle top located at 0 m. The values represent the average measurements taken at each reactor height. Overall, the furnace temperature evolution in the three experiments fell into the typical pattern described by a CFB combustor. This is characterized by stable temperatures in the upper part and a gradual temperature increase in the bottom region. While all three experiments indicated a similar temperature behavior in the upper part, the bottom section of the reactor introduced a distinct pattern at the OXY28 case. Please note that the riser temperature was controlled using a fluidized bed top heat exchanger during the latter test. Due to the limited length of the cooling rods (of approx. 5 m), the heat exchanger could only accommodate temperature fluctuations occurring in the upper half of the reactor. In consequence, the bottom-middle section of the riser experienced enhanced combustion conditions (up to 936 °C). This operation mode was

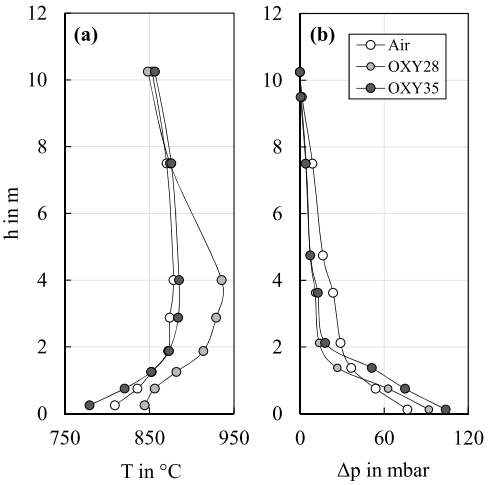

Figure 9. Temperature (T) (a) and pressure (Δp) (b) profiles along reactor height (h) at a reference boiler temperature of 880 °C.

maintained for several hours, although it ultimately led to bed material sintering and agglomeration issues. As for OXY35, a different approach was followed. Aiming at simulating a real fluidized bed cooler, the CFB reactor was coupled to a bubbling fluidized bed (BFB) reactor, setting the required process conditions to ensure smooth operation of the CFB reactor. For a detailed description of the proposed BFB−CFB reactor coupling please refer elsewhere.[27,52] As can be observed, the temperature distribution during OXY35 was very similar to the one obtained during air combustion conditions. This latter finding indicates that the advantages of increased inlet oxygen concentrations can be attained at the 200 kW$_{th}$ facility, providing that a uniform and sufficient cooling duty over the whole reaction height is guaranteed. Besides, the pressure profile described by the CFB reactor was similar in all investigated cases. Figure 9b displays a shaped curve in the bottom region with an almost linear gradient in the riser, indicating a uniform distribution of the bed inventory along with the reactor height. Minor differences were attained in the bottom section of the reactor (i.e., up to 2 m). While a pressure drop of 77 mbar was measured during air-firing conditions, differences up to 104 mbar were obtained under oxy-fuel combustion. With negligible differences in the solid bed inventory, the latter effect can be explained through a

https://doi.org/10.1021/acsomega.1c07334
ACS Omega 2022, 7, 8950−8959

reduction in the total flue gas volume flow with respect to air-firing. The results introduced in this section demonstrate the viability of employing a CFB combustor for the combustion of low-grade fuels, achieving stable hydrodynamic conditions both during air and oxy-fuel firing conditions. Particularly at oxy-fuel conditions, the riser temperature distribution has played a major role in the stability of the system. In line with the conclusions drawn by Stanger et al.,[21] the results included in this work have shown that temperatures below 1000 °C are required in the bottom section to avoid any risks associated with bed material sintering and agglomeration.

4. CONCLUSIONS

This work has analyzed the combustion behavior of SRF in a 200 kW_{th} CFB combustion facility operated under industrially relevant process conditions (TRL6). Dedicated investigations on the influence of temperature and combustion atmosphere have been devoted to characterizing the process in terms of gas pollutant formation and hydrodynamic stability. The behavior of NO_x upon combustion atmosphere and temperature correlates well with the conclusions drawn from previous studies. Compared to air-firing conditions, the volume concentration of NO_x significantly increased during oxy-fuel operation (by about 50%). At the same time, fuel-specific NO_x emissions decreased because of the absence of airborne nitrogen in combination with the reduced total gas volume flow. Besides, the process temperature posed a mild effect on the volume concentration of NO_x, under the premise that temperature was homogeneously distributed along with the reactor height. In parallel, both oxidant staging and dilution proved essential to avoid any localized hot spots within the boiler, thereby suppressing prompt and thermal NO_x formation. The concentration of SO_2 was particularly influenced by the presence of calcium-containing species in the fuel ash (by about 0.23 kg/kg) and was strongly inhibited at specific flue gas desulfurization temperatures (i.e., 871−880 °C). HCl emissions showed to be mainly promoted during oxy-fuel combustion due to enhanced metal vaporization and chlorination achieved by flue gas recirculation. Similar to y_{SO_2}, the concentration of HCl was shown to decrease within a temperature window of 871−880 °C due to the reduced availability of SO_2 required for alkali sulfation in combination with the ability of calcium-containing ash species to absorb HCl. In any case, the relatively high emissions of NO_x and HCl will most certainly require further treatment. NO_x can be easily removed during compression in the CPU in a high-pressure contact column, while HCl reduction can be achieved by dry sorbent injection. A smooth temperature profile in the riser proved to be essential to allow for the stable investigation of increased oxy-fuel cases. The pressure differences across the riser were comparable in all tests, with slightly higher pressure drops during oxy-fuel combustion due to the reduced total gas throughput. The results included in this study contribute to a better understanding of the fundamental oxy-fuel knowledge with alternative fuels and may serve to guide future process design and scale-up.

AUTHOR INFORMATION

Corresponding Author

Joseba Moreno − *University of Stuttgart, Institute of Combustion and Power Plant Technology (IFK), Stuttgart 70569, Germany*; orcid.org/0000-0002-6756-4404; Email: joseba.moreno@ifk.uni-stuttgart.de

Authors

Max Schmid − *University of Stuttgart, Institute of Combustion and Power Plant Technology (IFK), Stuttgart 70569, Germany*

Steven Scharr − *University of Stuttgart, Institute of Combustion and Power Plant Technology (IFK), Stuttgart 70569, Germany*

Günter Scheffknecht − *University of Stuttgart, Institute of Combustion and Power Plant Technology (IFK), Stuttgart 70569, Germany*

Complete contact information is available at: https://pubs.acs.org/10.1021/acsomega.1c07334

Author Contributions

CRediT authorship contribution statement. Joseba Moreno: Conceptualization, Methodology, Validation, Investigation, Data Curation, Writing − Original Draft, Visualization. Max Schmid: Review & Editing. Steven Scharr: Review & Editing. Günter Scheffknecht: Project Administration, Supervision, Review & Editing.

Funding

This publication has resulted from the joint ERA-NET Accelerating CCS Technologies (ACT2) research project "NEWEST-CCUS" (project no. 299683), with financial contribution from the German Federal Ministry of Economic Affairs and Climate Action (BMWK) (grant no. 03EE5020).

Notes

The authors declare no competing financial interest.

ACKNOWLEDGMENTS

The authors gratefully acknowledge the cooperation and support by the NEWEST-CCUS project partners. The authors are also grateful to the technical staff, academic colleagues, and research assistants of IFK's department "Decentralized Energy Conversion" for their assistance during the experiments. Finally, special thanks go to W. Roß and his team of IFK's "Laboratory for Fuels, Ashes, and Slag" for supporting this work with lab analyses of fuels and sorbents.

NOMENCLATURE

c_i	mass fraction of component "i" in gas (mg/m^3)
e_i	emission factor of component "i" in gas (mg/MJ$_{th}$)
h	height (m)
H_u	net calorific value (MJ/kg)
$\dot{M}$	mass flow (kg/h or kg/s)
$\dot{Q}$	heat flow (kW)
T	temperature (°C)
u_0	gas superficial velocity (m/s)
$\dot{V}$	volume flow (m^3/h, STP)
W_s	solid bed inventory (kg or kg/m^2)
x_i	mass fraction of component "i" in sorbent (kg/kg)
y_i	volume fraction of component "i" in gas (vol % or ppmv)

GREEK LETTERS

η_i	conversion ratio of component "i" (kg/kg)
Δp	pressure difference (mbar)
γ_i	mass fraction of component "i" in fuel (kg/kg)
ν	flue gas recirculation rate (%)
$\rho_{n,i}$	standard density of component "i" (kg/m^3)

https://doi.org/10.1021/acsomega.1c07334
ACS Omega 2022, 7, 8950−8959

ξ stoichiometric oxygen-to-fuel ratio (kg/kg)

■ ACRONYMS:

ASU air separation unit
BAT best available techniques
BECCS bio-energy combined with carbon capture and storage
BFB bubbling fluidized bed
CAPEX capital expenditures
CCS carbon capture and storage
CFB circulating fluidized bed
CPU (CO_2) compression and purification unit
DSI dry sorbent injection
OPEX operating expenditures
SRF solid recovered fuel
TRL technology readiness level

■ SUBSCRIPTS

ad air dried
FG flue gas
in inlet
out outlet
th thermal
waf water and ash free
wf water free

■ REFERENCES

(1) United Nations Treaty Collection. *The Paris Agreement*; Chapter XXVII 7 d, 2015.
(2) European Commision. *The Role of Waste-to-Energy in the Circular Economy*, 2017.
(3) Bui, M.; Fajardy, M.; Dowell, N. M. Thermodynamic Evaluation of Carbon Negative Power Generation: Bio-energy CCS (BECCS). *Energy Proc.* **2017**, *114*, 6010−6020.
(4) Gough, C.; Upham, P. Biomass energy with carbon capture and storage (BECCS or Bio-CCS). *Greenhouse Gases: Sci. Technol.* **2011**, *1*, 324−334.
(5) Ditaranto, M.; Becidan, M.; Stuen, J. Opportunities for CO_2 Capture in the Waste-to-Energy Sector. *Waste Management*; Thomé-Kozmiensky Verlag GmbH, 2019; Vol. *9*, pp 319−328.
(6) Wienchol, P.; Szlęk, A.; Ditaranto, M. Waste-to-energy technology integrated with carbon capture - Challenges and opportunities. *Energy* **2020**, *198*, 117352.
(7) Hofbauer, G. *Experimentelle Untersuchung der Oxy-Fuel-Verbrennung von Steinkohle in einer zirkulierenden Wirbelschichtfeuerung*; Universität Stuttgart, 2017 (DOI: 10.18419/opus-9129).
(8) Lupion, M.; Alvarez, I.; Otero, P.; Kuivalainen, R.; Lantto, J.; Hotta, A.; Hack, H. 30 MW_{th} CIUDEN Oxy-CFB Boiler-First Experiences. *Energy Proc.* **2013**, *37*, 6179−6188.
(9) Tan, Y.; Jia, L.; Wu, Y.; Anthony, E. J. Experiences and results on a 0.8MW_{th} oxy-fuel operation pilot-scale circulating fluidized bed. *Appl. Energy* **2012**, *92*, 343−347.
(10) Duan, L.; Duan, Y.; Zhao, C.; Anthony, E. J. NO emission during co-firing coal and biomass in an oxy-fuel circulating fluidized bed combustor. *Fuel* **2015**, *150*, 8−13.
(11) Sung, J.-H.; Back, S.-K.; Jeong, B.-M.; Kim, J.-H.; Choi, H. S.; Jang, H.-N.; Seo, Y.-C. Oxy-fuel co-combustion of sewage sludge and wood pellets with flue gas recirculation in a circulating fluidized bed. *Fuel Process. Technol.* **2018**, *172*, 79−85.
(12) Varol, M.; Symonds, R.; Anthony, E. J.; Lu, D.; Jia, L.; Tan, Y. Emissions from Co-firing Lignite and Biomass in an Oxy-fired CFBC. *Fuel Process. Technol.* **2018**, *173*, 126−133.
(13) Liu, Q.; Zhong, W.; Yu, H.; Tang, R.; Yu, A. Experimental Studies on the Emission of Gaseous Pollutants in an Oxy-Fuel-Fluidized Bed with the Cofiring of Coal and Biomass Waste Fuels. *Energy Fuels* **2020**, *34*, 7373−7387.
(14) Liu, Q.; Zhong, W.; Tang, R.; Yu, H.; Gu, J.; Zhou, G.; Yu, A. Experimental tests on co-firing coal and biomass waste fuels in a fluidised bed under oxy-fuel combustion. *Fuel* **2021**, *286*, 119312.
(15) Haaf, M.; Müller, A.; Unger, A.; Ströhle, J.; Epple, B. Combustion of solid recovered fuels in a semi-industrial circulating fluidized bed pilot plant - Implications of bed material and combustion atmosphere on gaseous emissions. *VGB PowerTech* **2020**, *3*, 51−56.
(16) Ikeda, M.; Toporov, D.; Christ, D.; Stadler, H.; Förster, M.; Kneer, R. Trends in NO_x Emissions during Pulverized Fuel Oxy-fuel Combustion. *Energy Fuels* **2012**, *26*, 3141−3149.
(17) Scheffknecht, G.; Al-Makhadmeh, L.; Schnell, U.; Maier, J. Oxy-fuel coal combustion-A review of the current state-of-the-art. *Int. J. Greenh. Gas Control* **2011**, *5*, S16−S35.
(18) Álvarez, L.; Gharebaghi, M.; Jones, J. M.; Pourkashanian, M.; Williams, A.; Riaza, J.; Pevida, C.; Pis, J. J.; Rubiera, F. CFD modeling of oxy-coal combustion: Prediction of burnout, volatile and NO precursors release. *Appl. Energy* **2013**, *104*, 653−665.
(19) Pang, L.; Shao, Y.; Zhong, W.; Gong, Z.; Liu, H. Experimental study of NO_x emissions in a 30 kW_{th} pressurized oxy-coal fluidized bed combustor. *Energy* **2020**, *194*, 116756.
(20) Krzywanski, J.; Czakiert, T.; Shimizu, T.; Majchrzak-Kuceba, I.; Shimazaki, Y.; Zylka, A.; Grabowska, K.; Sosnowski, M. NO_x Emissions from Regenerator of Calcium Looping Process. *Energy Fuels* **2018**, *32*, 6355−6362.
(21) Stanger, R.; Wall, T.; Spörl, R.; Paneru, M.; Grathwohl, S.; Weidmann, M.; Scheffknecht, G.; McDonald, D.; Myöhänen, K.; Ritvanen, J.; Rahiala, S.; Hyppänen, T.; Mletzko, J.; Kather, A.; Santos, S. Oxyfuel combustion for CO_2 capture in power plants. *Int. J. Greenh. Gas Control* **2015**, *40*, 55−125.
(22) Spliethoff, H. *Power Generation from Solid Fuels in Power Systems*; Springer, 2010 (DOI: 10.1007/978-3-642-02856-4).
(23) Lupiáñez, C.; Mayoral, M. C.; Díez, L. I.; Pueyo, E.; Espatolero, S.; Manuel Andrés, J. The role of limestone during fluidized bed oxy-combustion of coal and biomass. *Appl. Energy* **2016**, *184*, 670−680.
(24) Xie, Z.; Ma, X. HCl Emission Characteristics during the Combustion of Eucalyptus Bark. *Energy Fuels* **2014**, *28*, 5826−5833.
(25) Hou, H.; Li, S.; Lu, Q. Gaseous Emission of Monocombustion of Sewage Sludge in a Circulating Fluidized Bed. *Ind. Eng. Chem. Res.* **2013**, *52*, 5556−5562.
(26) Dieter, H.; Bidwe, A. R.; Varela-Duelli, G.; Charitos, A.; Hawthorne, C.; Scheffknecht, G. Development of the calcium looping CO_2 capture technology from lab to pilot scale at IFK, University of Stuttgart. *Fuel* **2014**, *127*, 23−37.
(27) Hornberger, M.; Moreno, J.; Schmid, M.; Scheffknecht, G. Experimental investigation of the calcination reactor in a tail-end calcium looping configuration for CO_2 capture from cement plants. *Fuel* **2021**, *284*, 118927.
(28) RAL-GZ 724. *Sekundärbrennstoffe—Gütesicherung*; RAL Deutsches Institut für Gütesicherung und Kennzeichnung e. V.: Münster, Germany, 2012.
(29) Sun, J.; Shen, Z.; Zeng, Y.; Niu, X.; Wang, J.; Cao, J.; Gong, X.; Xu, H.; Wang, T.; Liu, H.; Yang, L. Characterization and cytotoxicity of PAHs in $PM_{2.5}$ emitted from residential solid fuel burning in the Guanzhong Plain, China. *Environ. Pollut.* **2018**, *241*, 359−368.
(30) Sun, J.; Shen, Z.; Zhang, L.; Zhang, Q.; Lei, Y.; Cao, J.; Huang, Y.; Liu, S.; Zheng, C.; Xu, H.; Liu, H.; Pan, H.; Liu, P.; Zhang, R. Impact of primary and secondary air supply intensity in stove on emissions of size-segregated particulate matter and carbonaceous aerosols from apple tree wood burning. *Atmos. Res.* **2018**, *202*, 33−39.
(31) Kather, A.; Scheffknecht, G. The oxycoal process with cryogenic oxygen supply. *Die Naturwissenschaften* **2009**, *96*, 993−1010.
(32) Hu, Y.; Yan, J. Characterization of flue gas in oxy-coal combustion processes for CO_2 capture. *Appl. Energy* **2012**, *90*, 113−121.
(33) Nowak, P. *Combustion of Biomass and Solid Recovered Fuels on the Grate*; Universität Stuttgart, 2019 (DOI: 10.18419/opus-10749).

https://doi.org/10.1021/acsomega.1c07334
ACS Omega 2022, 7, 8950−8959

(34) Elorf, A.; Sarh, B. Excess air ratio effects on flow and combustion caracteristics of pulverized biomass (olive cake). *Case Stud. Therm. Eng.* **2019**, *13*, 100367.
(35) 13. BImSchV. *Verordnung über Großfeuerungs-, Gasturbinen- und Verbrennungsmotoranlagen*; Bundesministerium der Justiz und für Verbraucherschutz; Bundesamt für Justiz: Berlin, Germany, 2013.
(36) Haaf, M.; Hilz, J.; Peters, J.; Unger, A.; Ströhle, J.; Epple, B. Operation of a 1 MW_{th} calcium looping pilot plant firing waste-derived fuels in the calciner. *Powder Technol.* **2020**, *372*, 267−274.
(37) Shah, M.; Degenstein, N.; Zanfir, M.; Kumar, R.; Bugayong, J.; Burgers, K. Near zero emissions oxy-combustion CO_2 purification technology. *Energy Proc.* **2011**, *4*, 988−995.
(38) Senior, C. L.; Morris, W.; Lewandowski, T. A. Emissions and risks associated with oxyfuel combustion: state of the science and critical data gaps. *J. Air Waste Manage. Assoc.* **2013**, *63*, 832−843.
(39) Andersson, K.; Normann, F.; Johnsson, F.; Leckner, B. NO Emission during Oxy-Fuel Combustion of Lignite. *Ind. Eng. Chem. Res.* **2008**, *47*, 1835−1845.
(40) Pikkarainen, T.; Saastamoinen, J.; Saastamoinen, H.; Leino, T.; Tourunen, A. Development of 2nd Generation Oxyfuel CFB Technology - Small Scale Combustion Experiments and Model Development Under High Oxygen Concentrations. *Energy Proc.* **2014**, *63*, 372−385.
(41) Jia, L.; Tan, Y.; Wang, C.; Anthony, E. J. Experimental Study of Oxy-Fuel Combustion and Sulfur Capture in a Mini-CFBC. *Energy Fuels* **2007**, *21*, 3160−3164.
(42) Hofbauer, G.; Beisheim, T.; Dieter, H.; Scheffknecht, G. Experiences from Oxy-fuel Combustion of Bituminous Coal in a 150 kW_{th} Circulating Fluidized Bed Pilot Facility. *Energy Proc.* **2014**, *51*, 24−30.
(43) Moreno, J.; Hornberger, M.; Schmid, M.; Scheffknecht, G. Oxy-Fuel Combustion of Hard Coal, Wheat Straw, and Solid Recovered Fuel in a 200 kW_{th} Calcium Looping CFB Calciner. *Energies* **2021**, *14*, 2162.
(44) Chang, K. K.; Flagan, R. C.; Gavalas, G. R.; Sharma, P. K. Combustion of calcium-exchanged coals. *Fuel* **1986**, *65*, 75−80.
(45) Hu, Y.; Naito, S.; Kobayashi, N.; Hasatani, M. CO_2, NO_x and SO_2 emissions from the combustion of coal with high oxygen concentration gases. *Fuel* **2000**, *79*, 1925−1932.
(46) Spörl, R.; Maier, J.; Scheffknecht, G. Sulphur Oxide Emissions from Dust-fired Oxy-fuel Combustion of Coal. *Energy Proc.* **2013**, *37*, 1435−1447.
(47) Díez, L. I.; Lupiáñez, C.; Guedea, I.; Bolea, I.; Romeo, L. M. Anthracite oxy-combustion characteristics in a 90 kW_{th} fluidized bed reactor. *Fuel Process. Technol.* **2015**, *139*, 196−203.
(48) Jiao, F.; Chen, J.; Zhang, L.; Wei, Y.; Ninomiya, Y.; Bhattacharya, S.; Yao, H. Ash partitioning during the oxy-fuel combustion of lignite and its dependence on the recirculation of flue gas impurities (H_2O, HCl and SO_2). *Fuel* **2011**, *90*, 2207−2216.
(49) Allgurén, T.; Andersson, K. Chemical Interactions between Potassium, Sulfur, Chlorine, and Carbon Monoxide in Air and Oxy-fuel Atmospheres. *Energy Fuels* **2020**, *34*, 900−906.
(50) Xie, W.; Liu, K.; Pan, W.-P.; Riley, J. T. Interaction between emissions of SO_2 and HCl in fluidized bed combustors. *Fuel* **1999**, *78*, 1425−1436.
(51) Neuwahl, F.; Cusano, G.; Gómez Benavides, J.; Holbrook, S.; Roudier, S. *Best Available Techniques (BAT) reference document for waste incineration: Industrial Emissions Directive 2010/75/EU (Integrated Pollution Prevention and Control)*; Publications Office of the European Union: Luxembourg, Luxembourg, 2019.
(52) Moreno, J.; Hornberger, M.; Schmid, M.; Scheffknecht, G. Part-Load Operation of a Novel Calcium Looping System for Flexible CO_2 Capture in Coal-Fired Power Plants. *Ind. Eng. Chem. Res.* **2021**, *60*, 7320.

https://doi.org/10.1021/acsomega.1c07334
ACS Omega 2022, 7, 8950−8959